Generation of unusual branched long chain alkanes from hydrous pyrolysis of anammox bacterial biomass

CrossMark

Darci Rush [a,*], Andrea Jaeschke [a,1], Jan A.J. Geenevasen [b], Erik Tegelaar [c], Jos Pureveen [c], Michael D. Lewan [d], Stefan Schouten [a], Jaap S. Sinninghe Damsté [a]

[a] NIOZ Royal Netherlands Institute for Sea Research, Department of Marine Organic Biogeochemistry, P.O. Box 59, 1790 AB Den Burg, Texel, The Netherlands
[b] University of Amsterdam, van 't Hoff Institute for Molecular Sciences, NMR Department, P.O. Box 94720, 1090 GS Amsterdam, The Netherlands
[c] Shell Global Solutions International, Kessler Park 1, 2288 GS Rijswijk, The Netherlands
[d] U.S. Geological Survey, Box 25046, MS 977, Denver, CO 80225, USA

ARTICLE INFO

ABSTRACT

Anammox, the microbial anaerobic oxidation of NH_4^+ by NO_2^- to produce N_2, is recognised as a key process in the marine, freshwater and soil N cycles, and has been found to be a major sink for fixed inorganic N in the ocean. Ladderane lipids are unique anammox bacterial membrane lipids used as biomarkers for such bacteria in recent and past environmental settings. However, their fate during diagenesis and early catagenesis is not well constrained. In this study, hydrous pyrolysis experiments were performed on anammox bacterial biomass and the generated aliphatic hydrocarbons, present in oil generated at 220–365 °C, were analysed. A unique class of hydrocarbons was detected, and a representative component was isolated and rigorously identified using 2D nuclear magnetic resonance (NMR) spectroscopy. It consisted of C_{24} to C_{31} branched long chain alkanes with two internal ethyl and/or propyl substituents. The alkanes were generated above 260 °C, with maximum generation at 320 and 335 °C. Their stable carbon isotopic values were depleted in ^{13}C, similar to carbon isotope values of the original anammox lipids, indicating that they were thermal products generated from lipids of anammox bacterial biomass. A range of sediments from different geological periods where anammox may have been an important process was screened for the presence of these compounds as possible catagenetic products. They were not detected, either because the concentration was too low, or the sediments screened were too immature for them to have been generated, or because the artificially produced products of anammox lipids may not reflect the natural diagenetic and catagenetic products of ladderane lipids.

© 2014 Elsevier Ltd. All rights reserved.

1. Introduction

Anaerobic ammonium oxidation (anammox) is considered an important process in the global N cycle and may contribute 30–50% of fixed N loss from marine environments (Kuypers et al., 2005; Hamersley et al., 2007; Ward, 2013). It is the oxidation of NH_4^+ with NO_2^- as electron acceptor. Anammox bacteria have been shown to be responsible for the reaction (Mulder et al., 1995; Strous et al., 1999; Jetten et al., 2009, 2010), which is thought to take place in a specialised organelle-like structure, the anammoxosome

(van Niftrik et al., 2008a,b). This compartment is enclosed by a specific membrane of lipids composed of linearly concatenated cyclobutane moieties (Sinninghe Damsté et al., 2002a). These so-called ladderane lipids (I–V; Fig. 1) are unique to anammox bacteria and have been used as biomarkers for the presence of the anammox reaction in the natural environment (e.g. Kuypers et al., 2003; Jaeschke et al., 2009a, 2010; Wakeham et al., 2012). However, ladderane fatty acids (FAs) are transformed relatively quickly during sediment burial, as evident from sedimentary records (Jaeschke et al., 2009b; Rush et al., 2012) and artificial maturation experiments (Jaeschke et al., 2008; Rush et al., 2011). This is probably due to the cyclobutane moieties, which are highly strained and likely susceptible to structural rearrangement during diagenesis and catagenesis.

Lipids undergo structural alteration during sedimentary processes (i.e. hydrogenation, sulfurisation, oxidation and condensation; Gaskell and Eglinton, 1975; Sinninghe Damsté et al., 1989,

* Corresponding author. Present address: Newcastle University, School of Civil Engineering and Geosciences, Drummond Building, Newcastle-upon-Tyne NE1 7RU, UK. Tel.: +44 1912088501.
E-mail address: darci.rush@ncl.ac.uk (D. Rush).
[1] Present address: Alfred Wegener Institute for Polar and Marine Research, Am Alten Hafen 26, 27568 Bremerhaven, Germany.
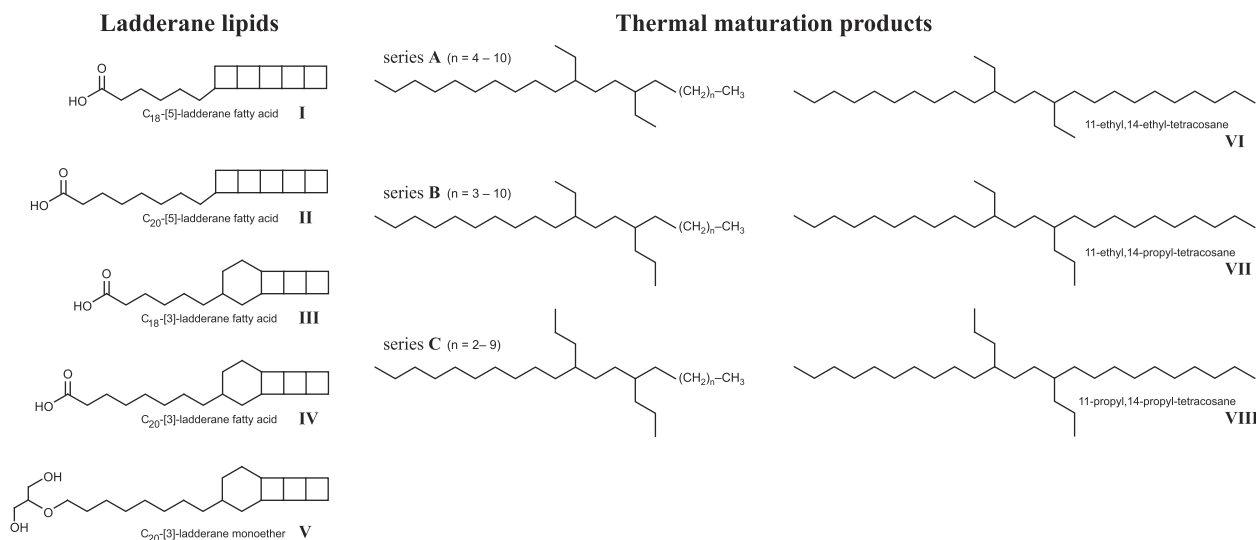
Fig. 1. Structures of ladderane lipids {(**I**) C_{18}-[5]-ladderane FA, (**II**) C_{20}-[5]-ladderane FA, (**III**) C_{18}-[3]-ladderane FA, (**IV**) C_{20}-[3]-ladderane FA and (**V**) C_{20}-[3]-ladderane monoether}, and maturation products in hydrous pyrolysates of anammox biomass [(**A**) Et–Et branched long chain alkane, (**B**) Et–Pr branched long chain alkane and (**C**) Pr–Pr branched long chain alkane]. The positions of the branching points remain constant. Chain length varies on one side of branching points (n = 2–10 carbons).

2002b; de Leeuw et al., 2006). Artificial maturation processes such as hydrous pyrolysis have been shown to simulate the generation of oil from organic-rich shales by heating them submerged in water in a closed reactor over a limited time period (up to one week) at temperatures in the range 280–370 °C (Lewan et al., 1979; Lewan, 1993). In addition to simulating catagenesis, hydrous pyrolysis has also been used to study the maturation of biomarkers (e.g. Koopmans et al., 1996; Schouten et al., 2004a) using temperatures < 280 °C. Jaeschke et al. (2008) used hydrous pyrolysis with anammox bacterial biomass to show that ladderane lipids underwent structural modification at low temperature (120 °C). The cyclobutane moieties of ladderane FAs and a ladderane monoether were shown to be opened, with concomitant formation of double bonds, resulting in several more stable components with condensed cyclohexenyl groups, in a process that had been observed for ladderane lipids during gas chromatography (GC) analysis (Sinninghe Damsté et al., 2005).

Here, we investigate the potential production of additional thermally stable biomarkers of anammox bacteria. We focussed on examining the aliphatic hydrocarbons since these components would likely be more stable than the ladderane FA lipids currently used as tracers for anammox, and it was hoped that they might be more suitable biomarkers for past anammox activity.

2. Material and methods

2.1. Hydrous pyrolysis

The conditions of the experiments have been described by Jaeschke et al. (2008). Briefly, 75 g of anammox bacterial biomass [*Candidatus Kuenenia stuttgartiensis*, making up to 70% of the bacterial population of the sludge of a wastewater treatment plant (Dokhaven, Rotterdam, The Netherlands); obtained from Paques B.V. (Balk, The Netherlands)] and 500 g distilled water were added to carburized 1 l Hastelloy-C276 reactors. Reactor contents were artificially matured at temperatures, which were kept constant, between 120 and 365 °C. After 72 h, the experiments were stopped and the reactors allowed to cool to room temperature within 24 h. The oils generated between 200 and 365 °C were recovered either from the water surface with a pipette, or from the reactor walls by rinsing with benzene.

2.2. Extraction and fractionation

An aliquot (3–10 mg) of the expelled oil was separated over a small Al_2O_3 columns with hexane, hexane/dichloromethane (DCM) (9:1; v/v), and DCM/MeOH (1:1; v/v). Saturated components were isolated from the hexane fraction by elution over an $AgNO_3$-impregnated silica column, using hexane as eluent. A known amount of internal standard (*anteiso* C_{22} alkane) was added to the hexane fraction for GC quantification, and the aliquot was air dried.

2.3. GC, GC–mass spectrometry (GC–MS) and GC–isotope ratio MS (GC–IRMS)

GC analysis was performed with a Hewlett–Packard (HP) 6890 instrument equipped with an on-column injector and flame ionisation detection (FID). A fused silica column (25 m × 0.32 mm) coated with CP Sil-5 (0.12 μm film thickness) was used with He as carrier gas. Samples were injected at 70 °C and the GC oven temperature was raised to 130 °C at 20 °C/min and then at 4 °C/min to 320 °C (held 15 min). GC–MS was carried out using a Finnigan Trace GC Ultra (Thermo Electron Corporation), interfaced with a Finnigan Trace DSQ mass spectrometer, with a range of m/z 50–800. GC conditions for GC–MS were as for GC. A selected alkane fraction (from the 320 °C experiment) was analysed using GC–MS under chemical ionisation (CI) conditions with CH_4 as collision gas, with a HP 5973 mass spectrometer and similar GC conditions.

Compound-specific carbon isotope ($\delta^{13}C$) analysis was carried out using a ThermoFinnigan DELTA-V irm GC–MS system. The column, carrier gas, and temperature programme conditions were the same as for GC analysis. The $\delta^{13}C$ values for the three most abundant components are reported in the standard δ per mil (‰) notation against Vienna Peedee Belemnite (Table 2). The performance of the instrument was checked daily with a mixture of perdeuteriated n-alkanes with known isotopic values.

2.4. Two dimensional (2D) GC–MS

2D GC–MS analysis was carried out on aliquots of the aliphatic hydrocarbon fraction of the oil expelled during the hydrous pyrolysis in order to separate, identify and quantify components which

co-eluted on GC-FID. 2D GC separation was achieved with a 'reversed set up' using an Agilent 7890 instrument. First, samples were injected on to a DB-17 ms column (20 m × 0.25 mm; 0.25 µm film thickness), at 40 °C (held 2 min). Oven temperature was raised at 2.5 °C/min to 300 °C (held 10 min). Plugs (10 s) were subsequently transferred to a second, nonpolar, DB-1 ms column (1.5 m × 0.1 mm; 0.1 µm film thickness). The 2D GC instrument was interfaced, at low ionisation (25 V), with a Jeol AccuTOF time-of-flight MS instrument (m/z 40–600).

2.5. GC–supersonic molecular beam (SMB)–MS (GC–SMB–MS)

The aliphatic hydrocarbon fraction from the 320 °C experiment was analysed using GC–SMB–MS. Analysis was performed with an Agilent 7890A GC instrument, coupled to an Agilent 5975C mass selective detector (MSD) with an Aviv Analytical 5975-SMB 101-09 SMB interface (cf. Fialkov et al., 2008). The sample was injected in splitless mode (injector 300 °C) at 50 °C on to a fused silica DB-1 column (60 m × 0.25 mm; 0.25 µm film thickness; He carrier gas). The oven temperature was increased to 320 °C (held 30 min) at 4 °C/min. He make up gas (35 ml/min) was used for cooling. Ionisation occurred in a fly-through dual cage electron ionisation (EI) source, at 70 eV. Full scan mode (m/z 50–650) was used.

2.6. Isolation of branched long chain alkane

A representative component of the branched long chain alkane series was isolated using preparative GC (prep-GC), in order to rigorously identify it by way of 1D and 2D nuclear magnetic resonance (NMR) spectroscopy. First, large aliquots (2–3 g) of expelled oil from the 280 and 300 °C hydrous pyrolysis experiments were

fractionated over large (25 cm × 2 cm) Al_2O_3 columns with hexane, hexane/DCM (9:1; v/v) and DCM/MeOH (1:1; v/v). The hexane fractions were cleaned up using large $AgNO_3$-impregnated silica columns. The resulting alkane fractions were combined and used for isolation of the component using an HP 6890 GC instrument coupled to a Gerstel Preparative Collector system. An aliquot (5 µl) of the purified fraction was injected at 70 °C by a HP 7683 series autoinjector, on to a CP-Sil 5 column (25 m × 32 mm, 0.52 µm film thickness). The GC temperature programme was run to 130 °C at 20 °C/min and then to 320 °C at 4 °C/min (held 10 min). A small fraction of the effluent was diverted for FID, while ca. 99% was sent to the preparative system. The contents of the fraction trap, cooled to 10 °C, were collected using DCM. Over a thousand injections were performed to trap sufficient material. The purity of the prepared fraction was determined using GC-FID.

2.7. 1D and 2D ^1H and ^{13}C NMR spectroscopy

The component isolated using prep-GC was sequentially dissolved and dried in (2×) DCM, (2×) $CHCl_3$, (2×) CCl_4 and (2×) $CDCl_3$ to remove residual proton signals from solvents, and then transferred to NMR tubes using 0.75 ml $CDCl_3$. 1D and 2D $^1H/^{13}C$ NMR analyses were performed with a Bruker DMX-600 spectrometer equipped with TCI cryoProbe and with a Bruker AV-750 with a 5 mm triple TXI-zGRAD probe, both at 298 K as reported by Sinninghe Damsté et al. (2005).

3. Results

Anammox bacterial biomass was previously artificially matured using hydrous pyrolysis in order to examine the effects of diagenesis

Table 1
Amount of recovered oil and branched hydrocarbons in artificially matured anammox biomass (based on 2D GC–MS quantification). Structures **VI–VIII** correspond to those in Fig. 1.[a]

Code	Name	n[d]	Hydrous pyrolysis temperature (°C)							
			200	220	280	300	320	335	350	365
Expelled oil/biomass (mg/g) Lipid yield (µg component/g original biomass)			1.8	2.0	35.5	43.3	52.4	55.3	42.3	22.6
338[b]A[c]	7-Ethyl,10-ethyleicosane	4	–[e]	–	< 1	1	6	4	3	2
338B	6-Propyl,9-ethylnonadecane	3	–	–	–	< 1	2	1	1	1
338C	5-Propyl,8-propyloctocosane	2	–	–	–	< 1	1	1	< 1	< 1
352A	8-Ethyl,11-ethylheneicosane	5	–	–	< 1	1	7	5	4	2
352B	7-Propyl,10-ethyleicosane	4	–	–	< 1	1	8	6	4	2
352C	6-Propyl,9-propylnonadecane	3	–	–	–	< 1	< 1	1	< 1	< 1
366A	9-Ethyl,12-ethyl-docosane	6	< 1	–	< 1	2	13	9	7	3
366B	8-Propyl,11-ethylheneicosane	5	–	–	< 1	2	7	6	4	2
366C	7-Propyl,10-propyleicosane	4	–	–	< 1	0	1	1	1	< 1
380A	10-Ethyl,13-ethyltricosane	7	< 1	–	< 1	2	5	4	3	1
380B	9-Propyl,12-ethyldocosane	6	< 1	–	< 1	3	13	11	7	3
380C	8-Popyl,11-propylheneicosane	5	–	–	< 1	< 1	1	2	1	1
394A (**VI**)	11-Ethyl,14-ethyltetracosane	8	< 1	< 1	6	21	27	31	16	6
394B	10-Propyl,13-ethyltricosane	7	–	–	< 1	2	5	5	3	1
394C	9-Propyl,12-propyldocosane	6	–	–	< 1	< 1	2	2	1	< 1
408A	11-Ethyl,14-ethylpentacosane	9	–	–	< 1	1	2	3	1	< 1
408B (**VII**)	11-Ethyl,14-propyltetracosane	8	< 1	< 1	8	29	39	44	22	7
408C	10-Propyl,13-propyltricosane	7	–	–	< 1	2	3	3	1	1
422A	11-eEhyl,14-ethylhexacosane	10	–	–	< 1	< 1	< 1	< 1	< 1	< 1
422B	11-Propyl,14-ethylpentacosane	9	–	–	< 1	< 1	1	1	1	< 1
422C (**VIII**)	11-Propyl,14-propyltetracosane	8	< 1	< 1	2	7	10	11	5	2
436B	11-Propyl,14-ethylhexacosane	10	–	–	< 1	1	4	4	2	1
436C	11-Propyl,14-propylpentacosane	9	–	< 1	< 1	< 1	< 1	< 1	< 1	< 1

[a] Pyrolysates from 240 °C and 260 °C were not analysed by way of 2D GC–MS; the only identifiable peak by way of GC–MS in either pyrolysate was **VII** (< 1 µg/g original biomass), detected in the 260 °C pyrolysate.
[b] Number, M[+].
[c] Letter, internal branching type (**A**, Et–Et; **B**, Et–Pr; **C**, Pr–Pr).
[d] Number of internal carbons on variable side of carbon skeleton chain (see Fig. 1).
[e] Not detected.

and catagenesis on anammox biomarker lipids (Jaeschke et al., 2008). Oil was generated from 200 to 365 °C (Table 1) and was analysed for aliphatic hydrocarbons, which may have contained potential thermally stable products of anammox bacterial lipids. GC–MS analysis of the aliphatic fraction of the oil (e.g. Fig. 2a) showed the presence of C_{29}–C_{35} hopanes and hopenes, as well as branched and straight chain C_{15}–C_{17} alkanes, which could be related to catagenetic products of conventional straight chain FAs, glycerol (di-)ethers,

9-methylhexadecanoic acid, 10-methylhexadecanoic acid and 9,14-dimethylhexadecanoic acid, present in anammox bacterial biomass (Sinninghe Damsté et al., 2005).

Above 260 °C, a cluster of unknown components was evident, eluting between C_{26} and C_{28} *n*-alkanes and before the C_{29}–C_{35} hopanes and hopenes (Fig. 2a; Table 1). This lipid class was not detected in the original anammox bacterial biomass (Jaeschke et al., 2008), indicating that the components were products formed
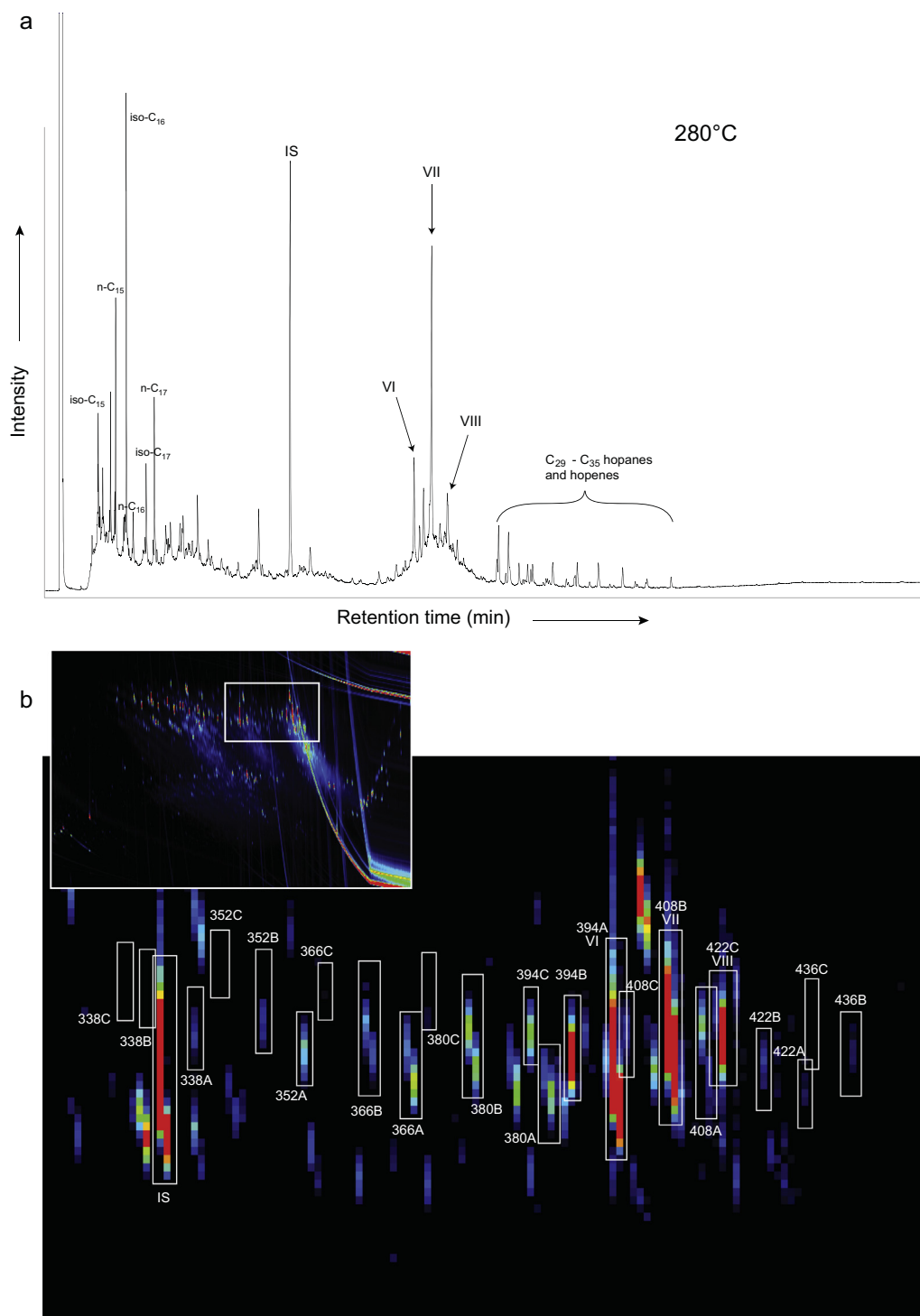

Fig. 2. Gas chromatograms of the aliphatic (hexane) fraction of the oil expelled during the 280 °C hydrous pyrolysis experiment. (a) GC-FID chromatogram, (b) enhanced area of 2D GC–GC chromatogram showing *m/z* 57 (alkane) filter. Inset shows full 2D GC–GC without mass filter. Roman numerals correspond to compounds in Fig. 1. Number and letter codes correspond to compounds in Table 1 [i.e. [a]number = M[+•], [b]letter = internal branching type (**A**, Et–Et; **B**, Et–Pr; **C**, Pr–Pr)]. IS, internal standard (*anteiso* C_{22} alkane).

via the thermal treatment. Stable carbon isotopic analysis revealed that they were ^{13}C depleted (−40.0‰ to −47.1‰; Table 2), similar to the original lipids of the unheated anammox bacterial biomass (ca. −48‰; Table 2), indicating that they likely derived from anammox bacterial biomass.

3.1. Identification of branched long chain alkanes

Three clearly distinguishable components were evident in the gas chromatogram of the saturated hydrocarbon fraction from the 280 °C experiment (**VI–VIII**; Fig. 2a). Their mass spectra were

Table 2
Stable carbon isotopic composition and retention indices of selected lipids in original anammox biomass and in oil generated from the hydrous pyrolysis (alkane fraction from 280 °C experiment; unheated and 200 °C data from single analyses by Jaeschke et al., 2008).

Lipid[a]	δ^{13}C (‰ vs. VPDB)			Kováts Index (silica)	
	Unheated	200 °C	280 °C	Observed	Calculated[b]
Iso-C$_{16}$ FAME[c]	−50.9	−49.4			
C$_{16}$:0 FAME[c]	−41.7	−42.0			
10-Methylhexadecanoic acid methyl ester	−44.8	−43.3			
IV	−48.9	−45.1			
V	−48.7	−45.4			
VI (**A**, n = 8)			−47.1 ± 0.1	2600	2610
VII (**B**, n = 8)			−41.8 ± 0.2	2665	2680
VIII (**C**, n = 8)			−40.0 ± 0.3	2731	2750

[a] Roman numerals correspond to structures in Fig. 1.
[b] According to Kissin and Feulmer (1986).
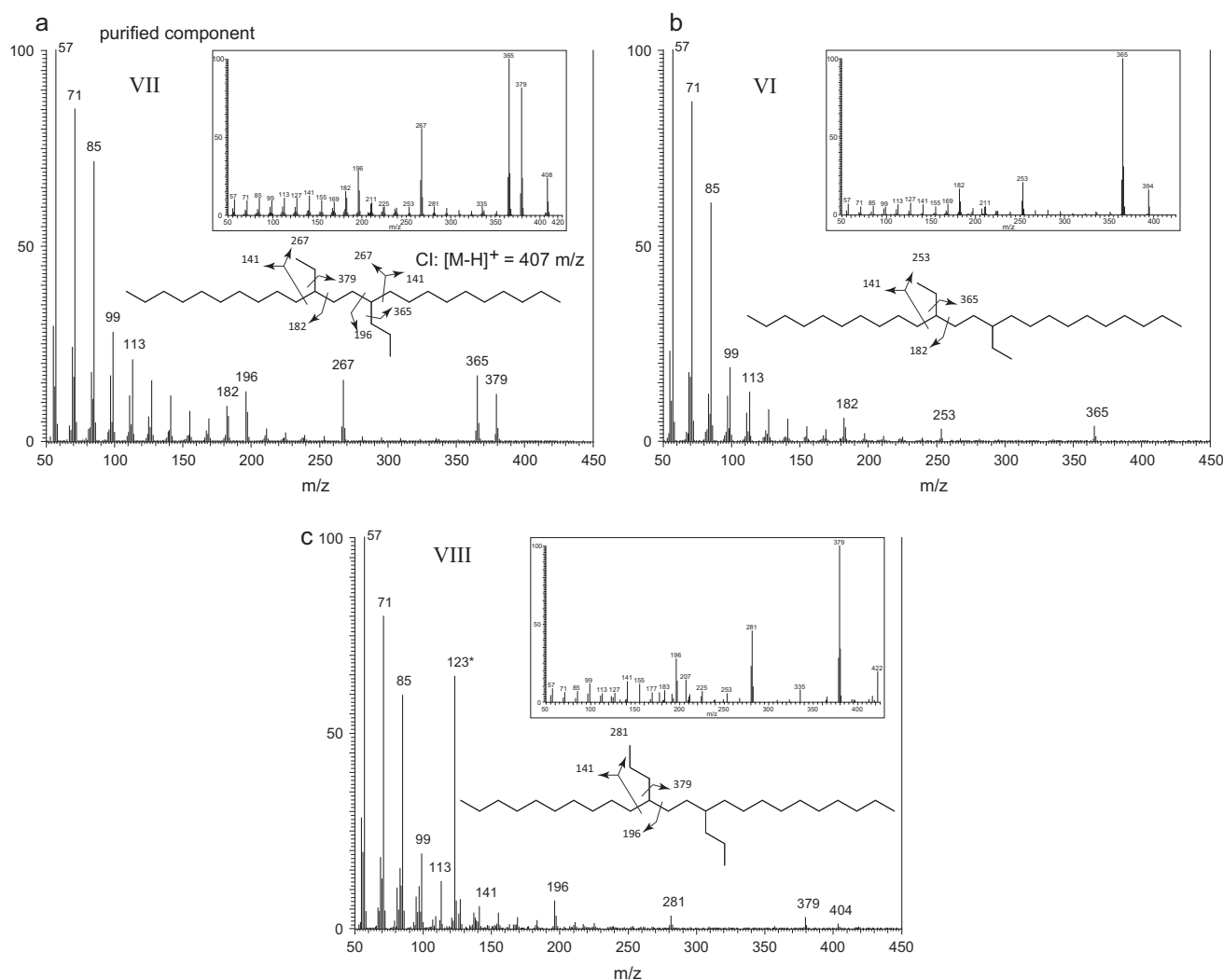[c] FAME, fatty acid methyl ester.

Fig. 3. Mass spectra (corrected for background) of branched hydrocarbons expelled during hydrous pyrolysis of anammox biomass: (a) **VII**, (b) **VI** and (c) **VIII** with corresponding structures [tentatively assigned for (b) and (c)]. Mass spectrum of (a) is from the isolated C$_{29}$ branched long chain alkane. [M−H]$^+$ for **VII** was determined from GC–CI–MS, and M$^{+\cdot}$ from GC–SMB–MS. Other spectra are from the alkane fraction of the oil generated at 320 °C. Insets show the spectra from GC–SMB–MS of the oil generated at 320 °C; *, impurity from co-eluting compound.

characterised by major fragments representative of alkanes (m/z 57, 71, 85, 99, etc.), as well as some even fragments (m/z 182 and 196) and fragment ions in the high m/z range at 253, 267, 281, 365, 379 (Fig. 3), suggesting that the components were branched alkanes.

3.1.1. Identification of 11-ethyl,14-propyltetracosane

The GC–MS spectrum of the most abundant branched alkane (Fig. 3a, **VII**) revealed characteristic elevated ions at m/z 182, 196, 267, 365 and 379. M[+•] was not observed in the EI spectrum, but [M−H][+] was detected as m/z 407 using GC–CI–MS, indicating a $C_{29}H_{60}$ alkane. The molecular mass was confirmed from GC–SMB–MS (M[+•] 408; Fig. 3a, inset), which also revealed the fragmentation related to the branching position in a more pronounced way. To elucidate its structure, the component was isolated using prep-GC (1.1 mg, GC purity of 96%), and studied by way of 1D and 2D NMR.

The attached proton test (APT) ^{13}C NMR spectrum (Table 3) revealed four primary carbons (i.e. methyl groups): two signals at 10.9 and 14.6 ppm, and a higher intensity signal at 14.1, probably representing two primary carbons. This was confirmed by the heteronuclear single quantum correlation spectroscopy (HSQC) experiment (Fig. 4), which showed that the chemical shift at 14.1 correlated with a triplet at 0.89 ppm in the ^{1}H NMR spectrum, representing six attached protons, and which was twice the intensity of the two other triplets at 0.84 and 0.88 ppm (Table 3). Furthermore, the APT ^{13}C NMR spectrum, in addition to a substantial number of secondary carbons, showed two tertiary carbons (37.54 and 39.24 ppm). The intensity of the signals at 14.1, 22.7, 31.9 ppm were twice the strength of most other signals, and are characteristic of carbons at the end of an *n*-alkyl chain. This, in combination with the presence of two additional methyls and two tertiary carbons (Table 4), indicated a dialkyl substituted *n*-alkyl chain. Since

the additional methyls were represented in the ^{1}H NMR spectrum as triplets, they must each have been connected to a secondary carbon. The heteronuclear multiple bond correlation (HMBC) experiment indicated that the triplet at 0.84 ppm showed connectivity with a secondary carbon at 39.24 ppm and a tertiary carbon at 25.93 ppm, establishing the presence of an Et group. Additionally, the triplet at 0.88 ppm showed connectivity with two secondary carbons (19.86 and 36.14 ppm), representing a Pr, or longer, alkyl moiety. The MS fragmentation (Fig. 3a) clearly revealed a loss of 29 Da (m/z 379; loss of Et) as well as 43 Da (m/z 365; loss of Pr), establishing both side chains. The position of the substituents (i.e. at C-11 and C-14; Fig. 3a) was also clearly indicated by fragment ions at m/z 182, 196 and 267, establishing the component as 11-ethyl,14-propyltetracosane (Fig. 3a, **VII**; Fig. 1, **B**, $n = 8$). Using the additivity principle for branched alkanes (Friebolin, 1991), the chemical shifts of the carbons were calculated and matched the observed shifts for an 11-ethyl,14-propyltetracosane (Table 2). The Kováts retention index (RI; Kováts, 1961) of the component was 2665 (silica), which is in agreement with the calculated RI value (2680), according to the equation of Kissin and Feulmer (1986).

3.1.2. MS assignment of other branched long chain alkanes

In addition to **VII**, two other components were detected with GC–MS, with similar spectra (**VI** and **VIII**; Fig. 3b and c, respectively). The fragments at m/z 182 and 253 (Fig. 3b) of **VI** suggested internal branching points at C-11 and C-14, likely with two Et substituents. The branching points for two Pr chains in component **VIII** were probably also at C-11 and C-14, based on the m/z 196 and 281 ions (Fig. 3c). M[+•] ions for **VI** and **VIII** were determined using GC–SMB–MS and found to be m/z 394 and m/z 422, respectively. The RIs for **VI** and **VIII** were 2600 and 2725 (silica), in agreement with the calculated RIs (2610 and 2750, respectively). Thus, the components

Table 3
1D and 2D ^{1}H and ^{13}C NMR data for **VII** (11-ethyl,14-propyltetracosane), formed during artificial maturation via hydrous pyrolysis.

.
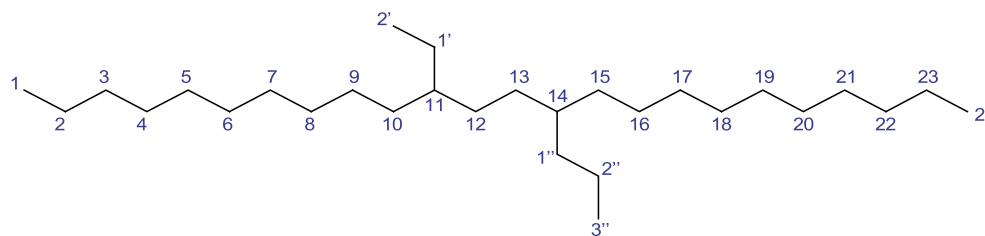
Carbon[a]	Proton shift (ppm)	Carbon shift (ppm)[a]			2D NMR correlations		Predicted C shift (ppm)[b]
		Primary	Secondary	Tertiary	COSY	HMBC	
1	0.89 (t, 3H)	14.11			2, 23	2, 23, 3, 22	14.1
2	1.27–1.30		22.69		1, 24		20.7
3	1.26		31.93				30.1
4–10	~1.3		~29.5				
11	1.17			39.24			38.2
12	1.22		33.20				32.8
13	1.22		33.67				33.2
14	1.25			37.54			35.8
15–21	~1.3		~29.5				
22	1.26		31.93				30.1
23	1.27–1.30		22.69		1, 24		20.7
24	0.89 (t, 3H)	14.11			2, 23	2, 23, 3, 22	14.1
1′	1.27		25.93		2′		28.0
2′	0.84 (t, 3H)	10.93			1′	1′, 11	12.0
1″	1.21		36.14		2″		37.4
2″	1.28		19.86		3″		18.6
3″	0.88 (t, 3H)	14.56			2″	2″,1″	14.5

[a] Carbon–proton connections established with an HSQC experiment.
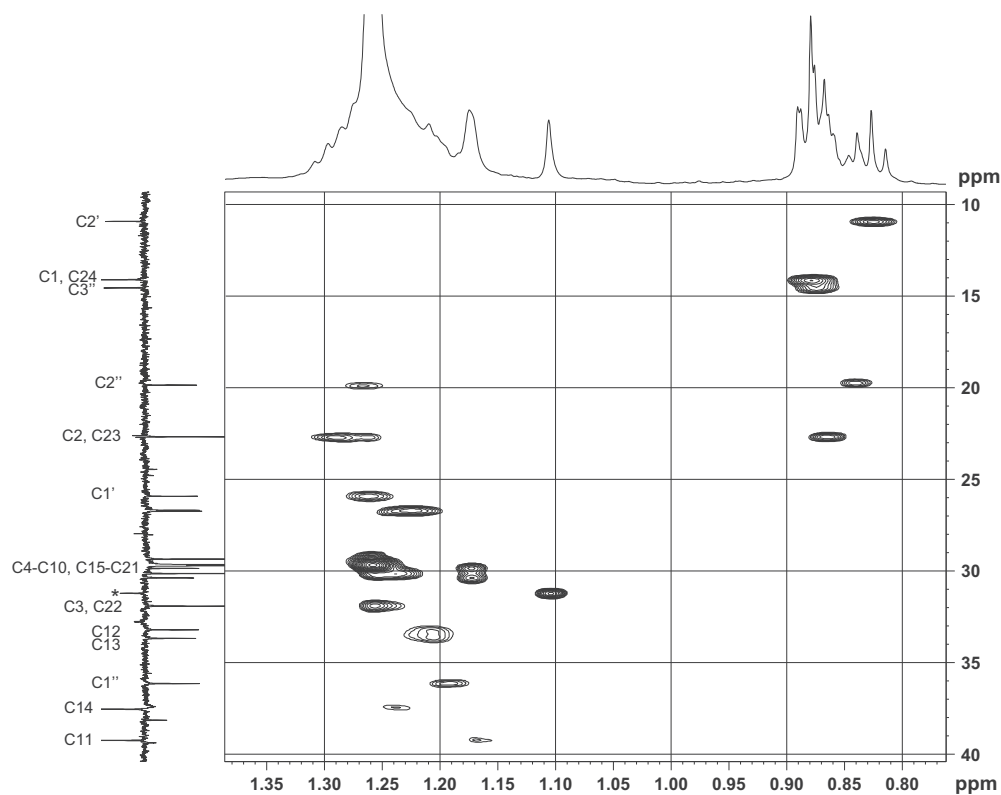[b] Calculated according to the additivity principle (Friebolin, 1991).

Fig. 4. HSQC for isolated component **VII**. Carbons are numbered according to assignments in Table 3; *, impurity.

Table 4
Sources of samples screened for thermally mature products of anammox biomass.

Sample origin	Samples screened	Age	Reference	Indication of maturity
Sapropel cores, Mediterranean	32	Pliocene	Menzel et al. (2005)	Shallow burial depth (50–80 mbsf)
Lomonosov Ridge, Arctic	30	Upper Eocene/Lower Paleocene	Schouten et al. (2007)	"Relatively high amount of C_{31} 17β,21β(H)-hopane"
Alpha Ridge, Arctic	5	Maastrichtian/Campanian	Jenkyns et al. (2004)	"> 80% of ββ-homohopane isomers"
Denmark	23	Paleocene–Eocene Thermal Maximum	Schoon et al. (2013)	Dominance of ββ-homohopane isomers
Walvis Ridge, South Atlantic	26	Turonian/Cenomanian	Forster et al. (2008)	"ββ/(ββ + αβ + βα) ratios for C_{31} > 0.6 (up to 0.9)"
Umbria, Italy	12	Cenomanian	Tsikos et al. (2004a)	
Furlo, Italy	4	Cenomanian	Forster et al. (unpublished)	
North-West Greece	6	Cenomanian/Albian	Tsikos et al. (2004b)	"Average T_{max} value 417 °C"
Demerara Rise, Tropical West Atlantic	6	Albian	Forster et al. (2004)	ββ/(ββ + αβ + βα) 0.6–0.9; for most samples, T_{max} was below or close to 400 °C
Mid Pacific Mountains	32	Aptian	van Breugel et al. (unpublished)	
Cismon Valley, Italy	35	Aptian	van Breugel et al. (2007)	ββ/(αβ + βα + ββ) 0.4–0.8
Paris Basin	4	Toarcian	van Breugel et al. (2006)	Free isorenieratane across entire section

were tentatively assigned as C_{28} 11-ethyl,14-ethyltetracosane (**VI**; Fig. 1, **A**, $n = 8$), and C_{30} 11-propyl,14-propyltetracosane (**VIII**; Fig. 1, **C**, $n = 8$), closely related to that of the unambiguously identified hydrocarbon **VII**.

3.1.3. Identification of long chain alkane series

2D GC–MS exposed a more complex pattern of branched long chain alkanes (Fig. 2b), which was not apparent in the initial investigation using 1D GC–MS (Fig. 2a). 2D GC–MS revealed that these unusual branched alkanes could be classified into three homologous series [**A** (Et–Et), **B** (Et–Pr) and **C** (Pr–Pr); Fig. 1] of C_{24} to C_{31} alkanes, of which **VI**, **VII**, and **VIII** (see above) were the most abundant members, respectively. They were tentatively assigned using MS by way of 2D GC–MS, which was supported by GC–SMB–MS (Table 1). In the series, the positions of the internal branch points remained constant, and chain length varied on only one side of the branch points (**n**, Fig. 1).

Fig. 5 shows two representative histograms of the concentration of branched long chain alkanes (from the 320 °C and 335 °C experiments). The distribution was the same across all temperatures. Series **B** (Et–Pr) was most abundant for all values of n, except for $n = 9$ (C_{25} alkyl carbon skeleton), where the Et–Et series (**A**) dominated, and for $n = 2$, where only one homologue of the **C** series was detected. Series **A** was the second most abundant. Branched
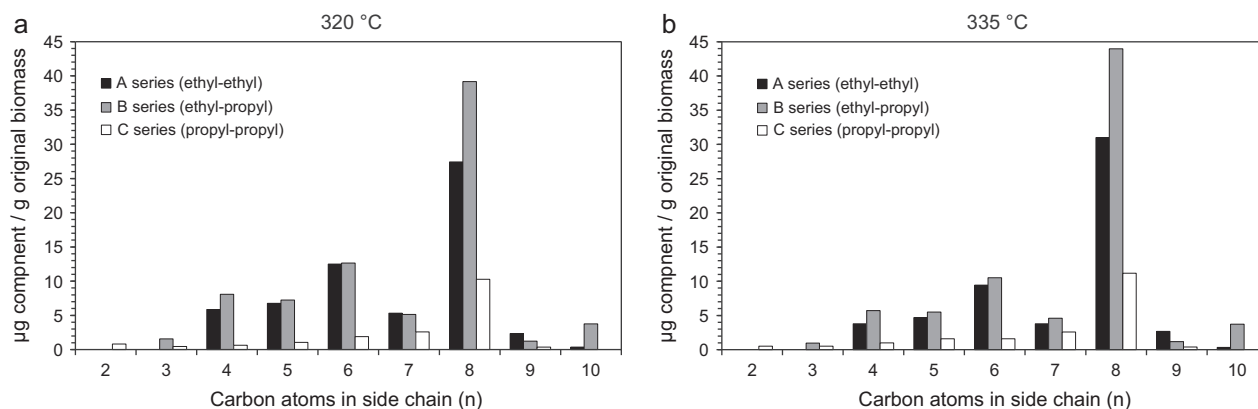
Fig. 5. Distribution of the three homologous series of branched alkanes from the (a) 320 °C and (b) 335 °C hydrous pyrolysis oil, showing similar types of distribution independent of internal substitution pattern. Quantification was based on integration of major fragment ions (i.e. branching points) in 2D GC–MS.

alkanes with $n = 8$ (C_{24} alkyl carbon skeleton; **VI**, **VII**, and **VIII**, Fig. 1) were always the most abundant members of all series.

4. Discussion

4.1. Generation and formation pathway of branched long chain alkanes

The alkanes were detected in the oil generated > 260 °C, with maximum abundances of the three most dominant (**VI**, **VII**, and **VIII**) at 335 °C (Fig. 6; Table 1). Branched long chain alkanes were the most dominant aliphatic hydrocarbons (Fig. 2) in the hydrous pyrolysis oils, which, along with their substantial depletion in ^{13}C [Table 2; cf. ^{13}C depletion of original ladderane lipids (Schouten et al., 2004b)], seems to indicate catagenetic products of anammox bacterial biomass. The products were also detected in the aliphatic fractions of the 260–350 °C residues analysed by Jaeschke et al. (2008), but were less abundant than in the oil (i.e. they were not the most abundant aliphatic hydrocarbons). It appears that branched long chain alkanes were preferentially expelled in the generated oil rather than retained in the residue, an effect seen in both natural primary migration and in hydrous pyrolysis experiments (Peters et al., 1990). The decline in concentration > 335 °C (Fig. 6) indicates that at higher temperatures branched long chain

alkanes are subject to thermal cracking, although no lower molecular weight hydrocarbons could be identified that could unambiguously be linked to the branched long chain alkanes.

Lipids with branched long chain alkyl carbon skeletons have not been reported before in anammox bacterial biomass. Furthermore, the chain lengths are substantially longer than those of the major ladderanes in anammox bacteria, i.e. C_{16}–C_{24} (Rattray et al., 2010). The distribution of these branched alkanes in the pyrolysates is rather specific, i.e. with **B** as the most abundant series, and with $n = 8$ as the most abundant side chain length (C_{24} alkyl carbon skeleton), and likely related to the original lipids from which the alkanes were formed. It is, however, difficult to imagine a degradation pathway from any identified anammox bacterial lipids (e.g. hydrocarbons, FAs, squalene or bacteriohopanepolyols; Sinninghe Damsté et al., 2005) that could account for the high number of carbons and specific branching pattern. It is therefore likely that they did not originate from known anammox bacterial lipids, but rather from other unknown lipids in the bacteria. Clearly, there is a need to reinvestigate the lipids of anammox bacterial biomass for biomolecules that could act as precursors for these unusual branched hydrocarbons upon thermal stress. It is possible that these lipids were not observed within the analytical window used in previous studies of anammox bacterial biomass lipids, which relied on GC–MS (Sinninghe Damsté et al., 2002a, 2005).

4.2. Environmental occurrence

The anammox process is limited to specific environmental conditions (O_2 depleted water column and/or sediments, containing NO_2^- and NH_4^+; Kuypers et al., 2003; Hamersley et al., 2007; Jaeschke et al., 2010; Wakeham et al., 2012). Therefore, we investigated sediments deposited during geological periods where anammox could have been an important process, i.e. ancient O_2 minimum zones and stratified anoxic basins. They were screened using GC–MS for the presence of the three most abundant components (**VI**, **VII**, and **VIII**; Table 4). However, none of the stable products of anammox lipids produced during hydrous pyrolysis could be detected. This might possibly be due to a low abundance of anammox lipids in environmental lipid mixtures. Anammox bacteria are slow growing Planctomycetes (Strous et al., 1999) and so comprise only a minor part of the microbial community in natural environments (Kuypers et al., 2005; Hamersley et al., 2007; Stevens and Ulloa, 2008; Podlaska et al., 2012). This means that the abundance of their lipids in the natural environment is low. For instance, the concentration of ladderane lipids in modern sediments is in the ng range (< 1–580 ng/g dry sediment; Jaeschke
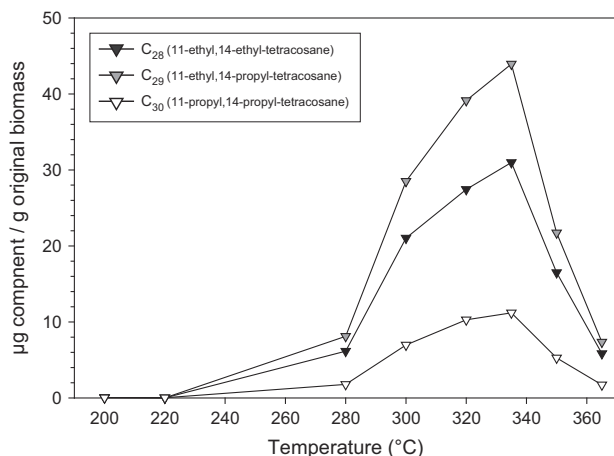

Fig. 6. Concentration (μg/g original anammox biomass) of the three most abundant (**VI–VIII**) branched long chain alkanes in oil generated as a function of hydrous pyrolysis temperature. The branched hydrocarbons were quantified from 2D GC–MS.

et al., 2009a,b, 2010; Rush et al., 2012), with an exceptional maximum of 4.9 µg/g sediment in one Arabian Sea core top (Rush et al., 2012). It is likely that the amount of thermally stable anammox bacterial lipid derivatives would be even lower in ancient sediments. Here, we used GC–MS, whereas to detect ladderanes in modern sediment samples a selective reaction monitoring triple quadrupole MS method is used (Hopmans et al., 2006). Therefore, our method is likely not sensitive enough and more sensitive methods such as 2D GC-time of flight-MS should be developed and tested.

A second explanation for the non-detection of these ladderane thermal products could be that the screened sediments were too immature. The 22S/(22S + 22R) ratio and the ββ/(αβ + βα + ββ) ratio of C_{31} homohopanes are often used as maturity indices (Seifert and Moldowan, 1980; van Duin et al., 1997). The maximum generation of this class of components was at relatively high hydrous pyrolysis temperatures (320–335 °C; Fig. 6). At these temperatures, the ββ/(αβ + βα + ββ) hopane ratio was 0 and the 22S/(22S + 22R) hopane ratio was ca. 0.4 (Jaeschke et al., 2008). This indicates that these conditions of hydrous pyrolysis correspond to those undergone by organic matter in thermally high mature sediments. Therefore, it is likely that the unusual branched alkanes are predominantly formed in sediments during catagenesis, when submitted to high thermal stress. Biomarker maturity parameters of the screened sediments indicated that they had not been exposed to this level of thermal stress, so these compounds may not yet have been generated (Table 4). Future screening of mature sediments and oils sourced from rocks deposited in anoxic basins using sensitive MS methods might reveal their presence.

Alternatively, the hydrous pyrolysis products may not reflect the natural degradation of anammox bacterial biomass. However, several studies have explored the discrepancies between natural petroleum formation and hydrous pyrolysis simulation and, although some dissimilarity is evident (e.g. Comet et al., 1986), most studies indicate that hydrous pyrolysis does mimic natural oil generation (Lewan, 1985, 1997; Peters et al., 1990; Koopmans et al., 1998).

5. Conclusions

Hydrous pyrolysis of anammox bacterial biomass resulted in the generation of a distinct lipid class: branched long chain alkanes (C_{24}–C_{31}). They are potential biomarkers of anoxia in the geological past. However, they were not detected in ancient sediments for periods where anammox could have been an important anaerobic pathway. This may be due to the possibility that they are not formed during natural maturation, the sediment samples screened were not thermally mature for these products to have been generated, or the method used was not sensitive enough. To test this, further studies using a more selective, multidimensional GC–MS technique with more mature sediments are needed. This study also showed that (polar) anammox lipids may have been overlooked during the original GC–MS screening of anammox biomass (Sinninghe Damsté et al., 2002b, 2005), as no known anammox lipid can be easily conceived as a precursor for the branched long chain alkanes. Future studies of anammox bacterial biomass should use different analytical tools besides GC–MS (e.g. full scan MS coupled to liquid chromatography, which is better suited for the detection of polar lipids).

Acknowledgements

Associate Editor—**P. Schaeffer**

References

Comet, P.A., McEvoy, J., Giger, W., Douglas, A.G., 1986. Hydrous and anhydrous pyrolysis of DSDP Leg-75 kerogens – a comparative study using a biological marker approach. Organic Geochemistry 9, 171–182.

de Leeuw, J.W., Versteegh, G.J.M., van Bergen, P.F., 2006. Biomacromolecules of algae and plants and their fossil analogues. Plant Ecology 182, 209–233.

Fialkov, A.B., Gordin, A., Amirav, A., 2008. Hydrocarbons and fuels analyses with supersonic gas chromatography mass spectrometry – the novel concept of isomer abundance analysis. Journal of Chromatography A 1195, 127–135.

Forster, A., Sturt, H., Meyers, P.A., Leg 207 Shipboard Scientific Party, 2004. Molecular biogeochemistry of Cretaceous black shales from the Demerara Rise: preliminary shipboard results from sites 1257 and 1258, LEG 207. Proceedings of the Ocean Drilling Program, Initial Reports 207, 1–21.

Forster, A., Kuypers, M.M.M., Turgeon, S.C., Brumsack, H.-J., Petrizzo, M.R., Sinninghe Damsté, J.S., 2008. The Cenomanian/Turonian oceanic anoxic event in the South Atlantic: new insights from a geochemical study of DSDP Site 530A. Palaeogeography, Palaeoclimatology, Palaeoecology 267, 256–283.

Friebolin, H., 1991. Basic One- and Two Dimensional NMR Spectroscopy. Wiley VCH Pub, Weinheim.

Gaskell, S.J., Eglinton, G., 1975. Rapid hydrogenation of sterols in a contemporary lacustrine sediment. Nature 254, 209–211.

Hamersley, M.R., Lavik, G., Woebken, D., Rattray, J.E., Lam, P., Hopmans, E.C., Sinninghe Damsté, J.S., Krüger, S., Graco, M., Gutiérrez, D., Kuypers, M.M.M., 2007. Anaerobic ammonium oxidation in the Peruvian oxygen minimum zone. Limnology and Oceanography 52, 923–933.

Hopmans, E.C., Kienhuis, M.V.M., Rattray, J.E., Jaeschke, A., Schouten, S., Sinninghe Damsté, J.S., 2006. Improved analysis of ladderane lipids in biomass and sediments using high-performance liquid chromatography/atmospheric pressure chemical ionization tandem mass spectrometry. Rapid Communications in Mass Spectrometry 20, 2099–2103.

Jaeschke, A., Lewan, M.D., Hopmans, E.C., Schouten, S., Sinninghe Damsté, J.S., 2008. Thermal stability of ladderane lipids as determined by hydrous pyrolysis. Organic Geochemistry 39, 1735–1741.

Jaeschke, A., Rooks, C., Trimmer, M., Nicholls, J.C., Hopmans, E.C., Schouten, S., Sinninghe Damsté, J.S., 2009a. Comparison of ladderane phospholipid and core lipids as indicators for anaerobic ammonium oxidation (anammox) in marine sediments. Geochimica et Cosmochimica Acta 73, 2077–2088.

Jaeschke, A., Ziegler, M., Hopmans, E.C., Reichart, G.-J., Lourens, L.j., Schouten, S., Sinninghe Damsté, J.S., 2009b. Molecular fossil evidence for anaerobic ammonium oxidation in the Arabian Sea over the last glacial cycle. Paleoceanography 24, PA2202-1–PA2202-11.

Jaeschke, A., Abbas, B., Zabel, M., Hopmans, E.C., Schouten, S., Sinninghe Damsté, J.S., 2010. Molecular evidence for anaerobic ammonium-oxidizing (anammox) bacteria in continental shelf and slope sediments off northwest Africa. Limnology and Oceanography 55, 365–376.

Jenkyns, H.C., Forster, A., Schouten, S., Sinninghe Damsté, J.S., 2004. High temperatures in the Late Cretaceous Arctic Ocean. Nature 432, 888–892.

Jetten, M.S.M., van Niftrik, L., Strous, M., Kartal, B., Keltjens, J.T., Op den Camp, H.J.M., 2009. Biochemistry and molecular biology of anammox bacteria. Critical Reviews in Biochemistry and Molecular Biology 44, 65–84.

Jetten, M.S.M., Op den Camp, H.J.M., Kuenen, J.G., Strous, M., 2010. Order II. "*Candidatus* Brocadiales". In: Krieg, N.R., Staley, J.T., Brown, D.R., Hedlund, B.P., Paster, B.J., Ward, N.L., Ludwig, W., Whitman, W.B. (Eds.), Bergey's Manual of Systematic Bacteriology, vol. 4. Springer, New York, USA, pp. 918, ISBN 979-0-387-95042-6.

Kissin, Y.V., Feulmer, G.P., 1986. Gas chromatographic analysis of alkyl-substituted paraffins. Journal of Chromatographic Science 24, 53–59.

Koopmans, M.P., De Leeuw, J.W., Lewan, M.D., Sinninghe Damsté, J.S., 1996. Impact of dia- and catagenesis on sulphur and oxygen sequestration of biomarkers as revealed by artificial maturation of an immature sedimentary rock. Organic Geochemistry 25, 391–426.

Koopmans, M.P., Rijpstra, W.I.C., De Leeuw, J.W., Lewan, M.D., Sinninghe Damsté, J.S., 1998. Artificial maturation of an immature sulfur and organic matter rich limestone from the Ghareb formation, Jordan. Organic Geochemistry 28, 503–521.

Kováts, E., 1961. Relation between structure and gas-chromatographic data for organic compounds. Fresenius' Zeitaschrift für Analitsche Chemie 181, 351–366.

Kuypers, M.M.M., Sliekers, A.O., Lavik, G., Schmid, M., Jørgensen, B.B., Kuenen, J.G., Sinninghe Damsté, J.S., Strous, M., Jetten, M.S.M., 2003. Anaerobic ammonium oxidation by anammox bacteria in the Black Sea. Nature 422, 608–611.

Kuypers, M.M.M., Lavik, G., Woebken, D., Schmid, M., Fuchs, B.M., Amann, R., Jørgensen, B.B., Jetten, M.S.M., 2005. Massive nitrogen loss from the Benguela upwelling system through anaerobic ammonium oxidation. Proceedings of the National Academy of Sciences of the United States of America 102, 6478–6483.

Lewan, M.D., 1985. Evaluation of petroleum generation by hydrous pyrolysis experimentation. Philosophical Transactions of the Royal Society of London Series A – Mathematical and Physical Sciences 315, 123–134.

Lewan, M.D., 1993. Laboratory simulation of petroleum formation: hydrous pyrolysis. In: Engel, M.H., Macko, S.A. (Eds.), Organic Geochemistry: Principles and Applications. Plenum Press, New York, pp. 419–442.

Lewan, M.D., 1997. Experiments on the role of water in petroleum formation. Geochimica et Cosmochimica Acta 61, 3691–3723.

Lewan, M.D., Winters, J.C., McDonald, J.H., 1979. Generation of oil-like pyrolyzates from organic-rich rhales. Science 203, 897–899.

Menzel, D., van Bergen, P.F., Veld, H., Brinkhuis, H., Sinninghe Damsté, J.S., 2005. The molecular composition of kerogen in Pliocene Mediterranean sapropels and associated homogeneous calcareous ooze. Organic Geochemistry 36, 1037–1053.

Mulder, A., Van de Graaf, A.A., Robertson, L.A., Kuenen, J.G., 1995. Anaerobic ammonium oxidation discovered in a denitrifying fluidized-bed reactor. FEMS Microbiology Ecology 16, 177–183.

Peters, K.E., Moldowan, J.M., Sundararaman, P., 1990. Effect of hydrous pyrolysis on biomarker thermal maturity parameters: Monterey phosphatic and siliceous members. Organic Geochemistry 15, 249–265.

Podlaska, A., Wakeham, S.G., Fanning, K.A., Taylor, G.T., 2012. Microbial community structure and productivity in the oxygen minimum zone of the eastern tropical North Pacific. Deep-Sea Research Part I 66, 77–89.

Rattray, J.E., van de Vossenberg, J., Jaeschke, A., Hopmans, E.C., Wakeham, S.G., Lavik, G., Kuypers, M.M.M., Strous, M., Jetten, M.S.M., Schouten, S., Sinninghe Damsté, J.S., 2010. Impact of temperature on ladderane lipid distribution in anammox bacteria. Applied and Environment Microbiology 76, 1596–1603.

Rush, D., Jaeschke, A., Hopmans, E.C., Geenevasen, J.A.J., Schouten, S., Sinninghe Damsté, J.S., 2011. Short chain ladderanes: oxic biodegradation products of anammox lipids. Geochimica et Cosmochimica Acta 75, 1662–1671.

Rush, D., Hopmans, E.C., Wakeham, S.G., Schouten, S., Sinninghe Damsté, J.S., 2012. Occurrence and distribution of ladderane oxidation products in different oceanic regimes. Biogeosciences 9, 2407–2418.

Schoon, P.L., Heilmann-Clausen, C., Schultz, B.P., Sluijs, A., Sinninghe Damsté, J.S., Schouten, S., 2013. Recognition of Early Eocene global carbon isotope excursions using lipids of marine Thaumarchaeota. Earth and Planetary Science Letters 373, 160–168.

Schouten, S., Hopmans, E.C., Sinninghe Damsté, J.S., 2004a. The effect of maturity and depositional redox conditions on archaeal tetraether lipid palaeothermometry. Organic Geochemistry 35, 567–571.

Schouten, S., Strous, M., Kuypers, M.M.M., Rijpstra, W.I.C., Baas, M., Schubert, C.J., Jetten, M.S.M., Sinninghe Damsté, J.S., 2004b. Stable carbon isotopic fractionations associated with inorganic carbon fixation by anaerobic ammonium-oxidizing bacteria. Applied and Environment Microbiology 70, 3785–3788.

Schouten, S., Woltering, M., Rijpstra, W.I.C., Sluijs, A., Brinkhuis, H., Sinninghe Damsté, J.S., 2007. The Paleocene–Eocene carbon isotope excursion in higher plant organic matter: differential fractionation of angiosperms and conifers in the Arctic. Earth and Planetary Science Letters 258, 581–592.

Seifert, C.J., Moldowan, J.M., 1980. The effect of thermal stress on source–rock quality as measured by hopane stereochemistry. Physics and Chemistry of the Earth 12, 229–237.

Sinninghe Damsté, J.S., Rijpstra, W.I.C., Kock-van Dalen, A.C., de Leeuw, J.W., Schenck, P.A., 1989. Quenching of labile functionalised lipids by inorganic sulphur species: evidence for the formation of sedimentary organic sulphur compounds at the early stages of diagenesis. Geochimica et Cosmochimica Acta 53, 1343–1355.

Sinninghe Damsté, J.S., Strous, M., Rijpstra, W.I.C., Hopmans, E.C., Geenevasen, J.A.J., Van Duin, A.C.T., Van Niftrik, L.A., Jetten, M.S.M., 2002a. Linearly concatenated cyclobutane lipids form a dense bacterial membrane. Nature 419, 708–712.

Sinninghe Damsté, J.S., Rijpstra, W.I.C., Reichart, G.J., 2002b. The influence of oxic degradation on the sedimentary biomarker record II. Evidence from Arabian Sea sediments. Geochimica et Cosmochimica Acta 66, 2737–2754.

Sinninghe Damsté, J.S., Rijpstra, W.I.C., Geenevasen, J.A.J., Strous, M., Jetten, M.S.M., 2005. Structural identification of ladderane and other membrane lipids of planctomycetes capable of anaerobic ammonium oxidation (anammox). FEBS Journal 272, 4270–4283.

Stevens, H., Ulloa, O., 2008. Bacterial diversity in the oxygen minimum zone of the eastern tropical South Pacific. Environmental Microbiology 10, 1244–1259.

Strous, M., Fuerst, J.A., Kramer, E.H.M., Logemann, S., Muyzer, G., van de Pas-Schoonen, K.T., Webb, R., Kuenen, J.G., Jetten, M.S.M., 1999. Missing lithotroph identified as new planctomycete. Nature 400, 446–449.

Tsikos, H., Jenkyns, H.C., Walsworth-Bell, B., Petrizzo, M.R., Forster, A., Kolonic, S., Erba, E., Silva, I.P., Baas, M., Wagner, T., Sinninghe Damsté, J.S., 2004a. Carbon-isotope stratigraphy recorded by the Cenomanian–Turonian Oceanic Anoxic Event: correlation and implications based on three key localities. Journal of the Geological Society 161, 711–719.

Tsikos, H., Karakitsios, V., van Breugel, Y., Walsworth-Bell, B., Bombardiere, L., Petrizzo, M.R., Sinninghe Damsté, J.S., Schouten, S., Erba, E., Premoli Silva, I., Farrimond, P., Tyson, R.V., Jenkyns, H.C., 2004b. Organic-carbon deposition in the Cretaceous of the Ionian basin, NW Greece. The Paquier Event (OAE 1b) revisited. Geological Magazine 141, 401–416.

van Breugel, Y., Baas, M., Schouten, S., Mattioli, E., Sinninghe Damsté, J.S., 2006. Isorenieratane record in black shales from the Paris Basin, France: constraints on recycling of respired CO_2 as a mechanism for negative carbon isotope shifts during the Toarcian oceanic anoxic event. Paleoceanography 21, PA4220-1–PA4220-8.

van Breugel, Y., Schouten, S., Tsikos, H., Erba, E., Price, G.D., Sinninghe Damsté, J.S., 2007. Synchronous negative carbon isotope shifts in marine and terrestrial biomarkers at the onset of the early Aptian oceanic anoxic event 1a: evidence for the release of ^{13}C-depleted carbon into the atmosphere. Paleoceanography 22, PA1210-1–PA1210-13.

van Duin, A.C.T., Sinninghe Damsté, J.S., Koopmans, M.P., van de Graaf, B., de Leeuw, J.W., 1997. A kinetic calculation method of homohopanoid maturation: application in the reconstruction of burial histories of sedimentary basins. Geochimica et Cosmochimica Acta 61, 2409–2429.

van Niftrik, L., Geerts, W.J.C., van Donselaar, E.G., Humbel, B.M., Yakushevska, A., Verkleij, A.J., Jetten, M.S.M., Strous, M., 2008a. Combined structural and chemical analysis of the anammoxosome: a membrane-bounded intracytoplasmic compartment in anammox bacteria. Journal of Structural Biology 161, 401–410.

van Niftrik, L., Geerts, W.J.C., van Donselaar, E.G., Humbel, B.M., Webb, R.I., Fuerst, J.A., Verkleij, A.J., Jetten, M.S.M., Strous, M., 2008b. Linking ultrastructure and function in four genera of anaerobic ammonium-oxidizing bacteria: cell plan, glycogen storage, and localization of cytochrome c proteins. Journal of Bacteriology 190, 708–717.

Wakeham, S.G., Turich, C., Schubotz, F., Podlaska, A., Li, X.N., Valera, R., Astor, Y., Saenz, J.P., Rush, D., Sinninghe Damsté, J.S., Summons, R.E., Scranton, M.I., Taylor, G.T., Hinrichs, K.-U., 2012. Biomarkers, chemistry and microbiology show chemoautotrophy in a multilayer chemocline in the Cariaco Basin. Deep-Sea Research I 63, 133–156.

Ward, B.B., 2013. How nitrogen is lost. Science 341, 352–353.